New Journal of Chemistry

Electronic Supplementary Information (ESI)

Two Azo-functionalized Luminescent 3D Cd(II)-MOFs for Highly Selective Detection of Fe^{3+} and Al^{3+}

Santanu Chand,[a] Manas Mandal,[a] Shyam Chand Pal,[a] Arun Pal,[a] Sinchan Maji,[b] Debaprasad Mandal[b] and Madhab C. Das[a]*

[a]*Department of Chemistry, Indian Institute of Technology Kharagpur, WB, 721302, India*
[b]*Department of Chemistry, Indian Institute of Technology Ropar, Punjab, 140001, India*
E-mail: mcdas@chem.iitkgp.ac.in

Physical Measurements. The FT-IR spectra were recorded from KBr pellets in the range of 400-4000 cm^{-1} on a Perkin-Elmer RX1 spectrophotometer. PXRD patterns were recorded using Cu K_α radiation (1.5418 Å) on a Bruker D8 Advance diffactometer. Thermogravimetric analysis (TGA) was performed using a TG 209 *F3* Tarsus (Netzsch) and the sample was heated from room temperature to 800 ^oC at a rate of 5 ^oC min^{-1} under N_2 atmosphere. ^1H, ^{13}C-NMR spectrum was recorded using a Bruker Avance II 400 spectrometer. Mass (MALDI-TOF) spectrum was recorded using a Bruker MALDI-TOF/TOF mass spectrometer. The luminescence spectra for the powdered solid samples were measured at room temperature using a Horiba Fluorolog spectrophotometer and the solution state fluorescence spectra were recorded using a Shimadzu-RF-6000 spectrophotometer. The UV−Vis spectra for the salt and small organic solvents solutions were measured at room temperature using a Shimadzu UV-2600 UV-Vis spectrophotometer. The morphology and elemental analysis of the samples were examined on a CarlZeiss MERLIN field emission scanning electron microscopy (FESEM) equipped with energy dispersive X-ray spectroscopy (EDX).

Single Crystal X-ray Diffraction. The crystal and refinement data for **1** and **2** were collected in Table S1. In this case, a crystal of appropriate size was selected from the mother liquor and immersed in paratone oil and then it was mounted on the tip of a glass fibre and cemented using epoxy resin. Single crystal X-ray data were collected at 300 K on a Bruker SMART APEX II CCD diffractometer using graphite-monochromated Mo-K_α radiation (0.71073 Å).

The linear absorption coefficients, scattering factors for the atoms and the anomalous dispersion corrections were taken from International Tables for X-ray Crystallography. The data integration and reduction were processed with SAINT[1] software. An empirical absorption correction was applied to the collected reflections with SADABS using XPREP.[2] The structure was solved by the direct method using SHELXTL[3] and was refined on F^2 by full-matrix least-squares technique using the SHELXL-2014[4] program package. For all the cases non-hydrogen atoms were refined anisotropically. Attempts to identify the highly disordered solvent molecules for **Cd-MOF-1** was failed. Instead, a new set of F^2 (hkl) values with the contribution from the solvent molecules withdrawn was obtained by the SQUEEZE procedure implemented in PLATON. [5] Selected bond lengths and bond angles are listed in Table S3 and S5.

Synthesis of 3,3'-azobis(pyridine) (L). The ligand L [3,3'-azobis(pyridine)] was synthesized based on a published methods.[12a, 12c in main text] A solution of 3-aminopyridine (12 g, 98%, 0.128 mol) in DI water (240 mL) was added drop wise into a two-neck round bottom flask containing 1.6 L of sodium hypochlorite (10-14wt %, NaOCl, being chilled in ice-water bath and magnetically stirred) over a period of 1 hr. The mixture was stirred at 0°C for another 30 min before the orange-coloured precipitate was filtered and the filtrate extracted with chloroform (200 mL× 3). The combined organic layers were dried over magnesium sulphate, then filtrated and remove the solvent, the corresponding crude product was purified by column chromatography on silica gel (ethyl acetate) to afford. The pure product was obtained as an orange-coloured, crystalline solid (needle shaped crystals, 7.32 g, 64% yield based on 4-aminopyridine). ^{1}H NMR (400MHz, $CDCl_3$): δ 9.23 (s, 2H), 8.74 (d, 2H), 8.17(d, 2H), 7.47(dd, 2H).^{13}C NMR (400MHz, $CDCl_3$): δ 152.1, 147.5, 140.9, 126.6, 123.8. FT-IR (KBr pellet, cm^{-1}): 3855(w), 3437.9(b), 2923(m), 2372.1(w), 1587(s), 1469(m), 1421(s), 1317(m), 1232(m), 1191.6(s), 1088(s), 1017.7(s), 958.4(m), 821.5(s), 699(s), 625(s), 547.7(m), 521.8(s).

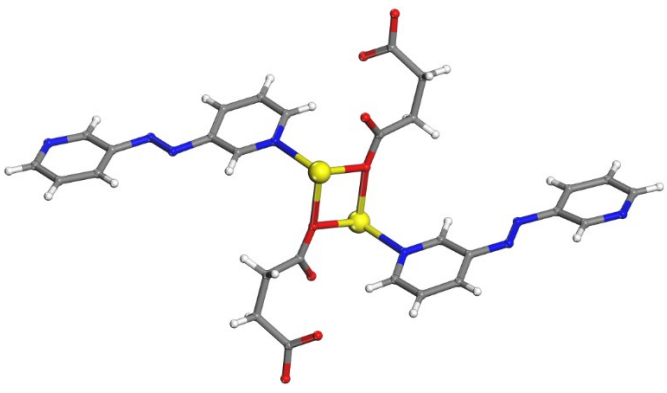

Fig. S1 Asymmetric unit of **Cd-MOF-1**. Color code: Cd, yellow; N, blue; O, red; C, grey; H, white.

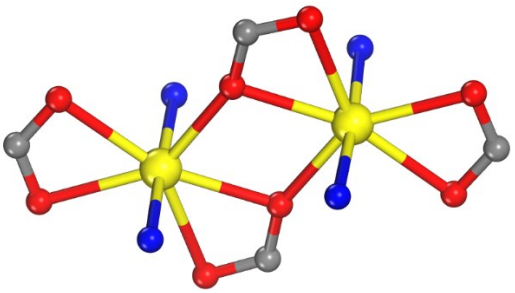

Fig. S2 Core View of **Cd-MOF-1**. Color code: Cd, yellow; N, blue; O, red; C, grey; H atoms are omitted for clarity.

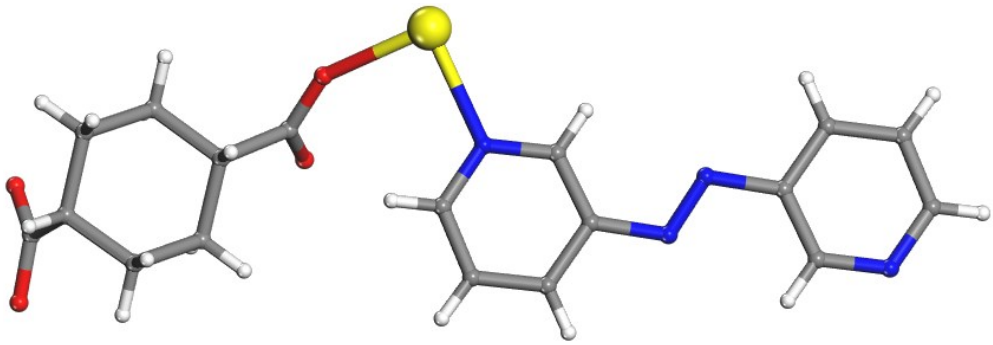

Fig. S3 Asymmetric unit of **Cd-MOF-2**. Color code: Cd, yellow; N, blue; O, red; C, grey; H, white.

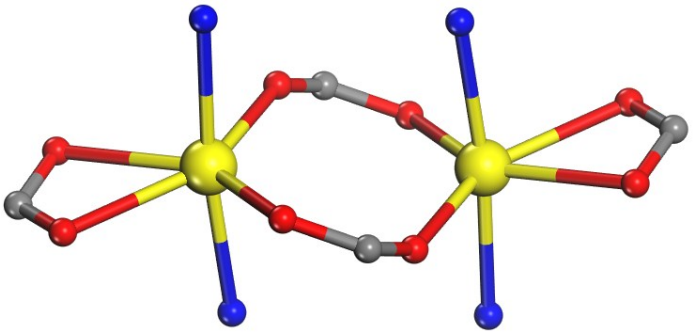

Fig. S4 Core View of **Cd-MOF-1**. Color code: Cd, yellow; N, blue; O, red; C, grey; H atoms are omitted for clarity.

Table S1: Crystal data and structure refinements for **Cd-MOF-1** and **Cd-MOF-2**.

	Cd-MOF-1	**Cd-MOF-2**
Empirical formula	$C_{28}\ H_{24}\ Cd_2\ N_8\ O_8$	$C_{18}\ H_{18}\ Cd\ N_4\ O_4$
Formula weight	825.35	466.76
Temperature(K)	293(2)	293(2)
Radiation	Mo (k_α)	Mo (k_α)
Wavelength(λ)	0.71073	0.71073
Crystal system	Monoclinic	Monoclinic
Space group	$P\ 2_1/n$	$P\ 2_1/n$
a[Å]	13.680(4)	11.265(2)
b[Å]	10.906(12)	13.097(3)
c[Å]	20.884(3)	12.563(3)
α[°]	90.00	90.00
β[°]	92.26(2)	106.74(3)
γ[°]	90.00	90.00
Volume[Å^3]	3113(4)	1775.0(7)
Z	4	4
Density (calculated) [Mg/m^3]	1.761	1.747
Absorption coefficient [mm-1]	1.428	1.263
F(000)	1632	963
Refl. used [$I > 2\sigma(I)$]	5705	3563
Independent reflections	6355	3649
Refinement method	full-matrix least squares on F^2	full-matrix least squares on F^2
GOF	1.054	1.120
Final R indices[I>2σ(I)]	R_1=0.0535 wR_2=0.1268	R_1=0.0169 wR_2=0.0429
R indices (all data)	R_1=0.0580 wR_2=0.1294	R_1=0.0175 wR_2=0.0432

Topology study

1. **Cd-MOF-1**

####################

1:C28 H20 Cd2 N8 O10

####################

Structure consists of molecules (ZD1). The composition of molecule is C2O2Cd2

Topology for ZD1

Atom ZD1 links by bridge ligands and has

Common vertex with R(A-A) f Total SA

ZD 1 0.0003 1.1953 0.2492 (0 0 0) 8.740A 1 10.63

ZD 1 0.0003 0.1953 0.2492 (0-1 0) 8.740A 1 15.37

ZD 1 1.0003 0.1953 0.2492 (1-1 0) 8.755A 1 10.88

ZD 1 1.0003 1.1953 0.2492 (1 0 0) 8.755A 1 15.51

Common edge with R(A-A)

ZD 1 0.5003 0.3047 -0.2508 (1 1 0) 11.311A 2 23.71

ZD 1 0.5003 1.3047 0.7492 (1 2 1) 12.347A 2 23.90

Structural group analysis

Structural group No 1

Structure consists of 3D framework with ZD

Coordination sequences

ZD1: 1 2 3 4 5 6 7 8 9 10

Num 6 22 52 94 148 214 292 382 484 598

Cum 7 29 81 175 323 537 829 1211 1695 2293

TD10=2293

Vertex symbols for selected sublattice

ZD1 Point symbol:{4^8.6^6.8}

Extended point symbol:[4.4.4.4.4.4.4.4.6(6).6(6).6(9).6(9).6(9).6(9).8(66)]

Point symbol for net: {4^8.6^6.8}

6-c net; uninodal net

Topological type: rob (topos&RCSR.ttd) {4^8.6^6.8} - VS [4.4.4.4.4.4.4.4.6(4).6(4).6(8).6(8).6(8).6(8).*] (16813 types in 3 databases)

Elapsed time: 2.72 sec.

2. Cd-MOF-2

##################

1:C18 H18 Cd N4 O4

##################

Structure consists of molecules (ZD1). The composition of molecule is C2Cd2

Topology for ZD1

Atom ZD1 links by bridge ligands and has

Common vertex with					R(A-A)	f	Total SA
ZD 1	1.0000	1.0000	1.0000	(1 0 1)	9.679A	1	10.72
ZD 1	0.0000	0.0000	0.0000	(0-1 0)	9.679A	1	10.72
ZD 1	0.0000	1.0000	0.0000	(0 0 0)	9.679A	1	15.71
ZD 1	1.0000	0.0000	1.0000	(1-1 1)	9.679A	1	15.71

Common edge with					R(A-A)		
ZD 1	1.5000	0.5000	0.5000	(1 0 0)	11.265A	2	23.56
ZD 1	-0.5000	0.5000	0.5000	(-1 0 0)	11.265A	2	23.56

Structural group analysis

Structural group No 1

Structure consists of 3D framework with ZD

Coordination sequences

ZD1: 1 2 3   4   5   6   7   8   9   10

Num   6 18 38 66 102 146 198 258 326 402

Cum   7 25 63 129 231 377 575 833 1159 1561

TD10=1561

Vertex symbols for selected sublattice

ZD1 Point symbol:{4^12.6^3}

Extended point symbol:[4.4.4.4.4.4.4.4.4.4.4.6(4).6(4).6(4)]

Point symbol for net: {4^12.6^3}

6-c net; uninodal net

Topological type: pcu alpha-Po primitive cubic; 6/4/c1; sqc1 (topos&RCSR.ttd) {4^12.6^3} - VS [4.4.4.4.4.4.4.4.4.4.4.*.*.*] (16813 types in 3 databases)

Elapsed time: 3.72 sec.

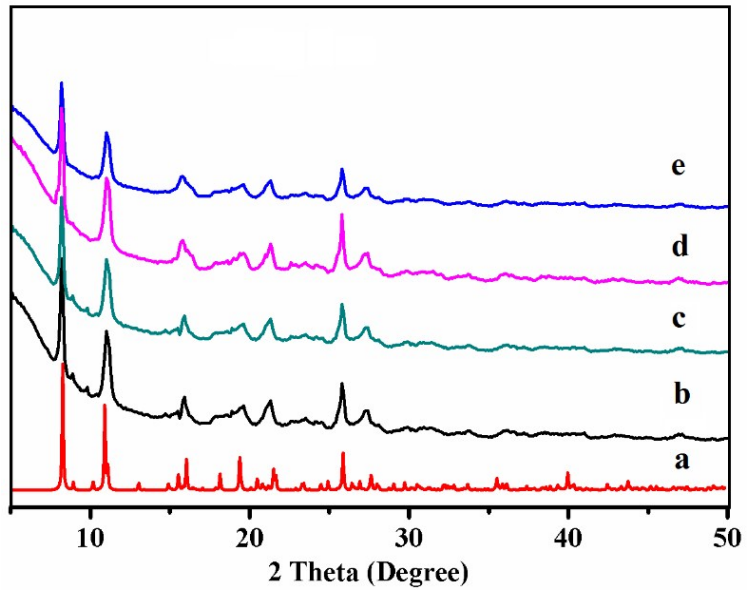

Fig. S5 The PXRD pattern of simulated (a), as synthesized sample **Cd-MOF-1** (b), after treated the sample with DMF (4 mL) and water (1mL) for 12 hours (c), after the sensing experiment of Fe^{3+} in DMF/water solution (d), after the sensing experiment of Al^{3+} in DMF/water solution of **Cd-MOF-1** (e).

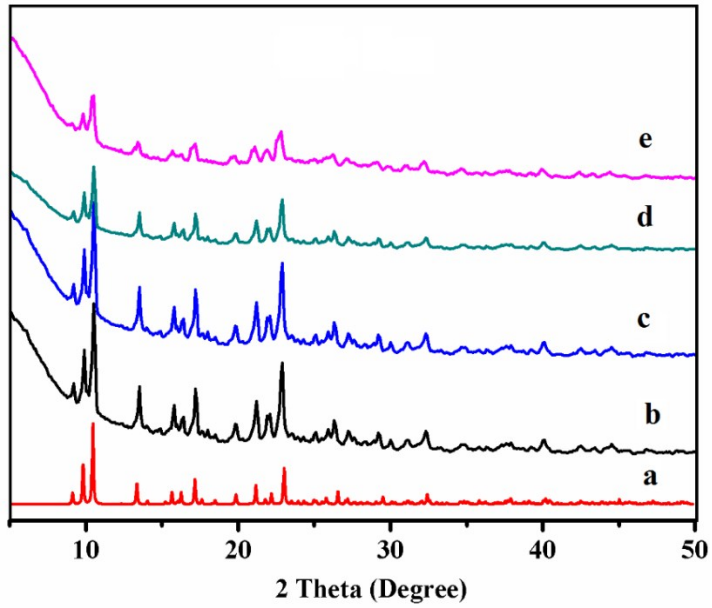

Fig. S6 The PXRD pattern of simulated (a), as synthesized sample **Cd-MOF-2** (b), after treated the sample with DMF (4 mL) and water (1mL) for 12 hours (c), after the sensing experiment of Fe^{3+} in DMF/water solution (d), after the sensing experiment of Al^{3+} in DMF/water solution of **Cd-MOF-2** (e).

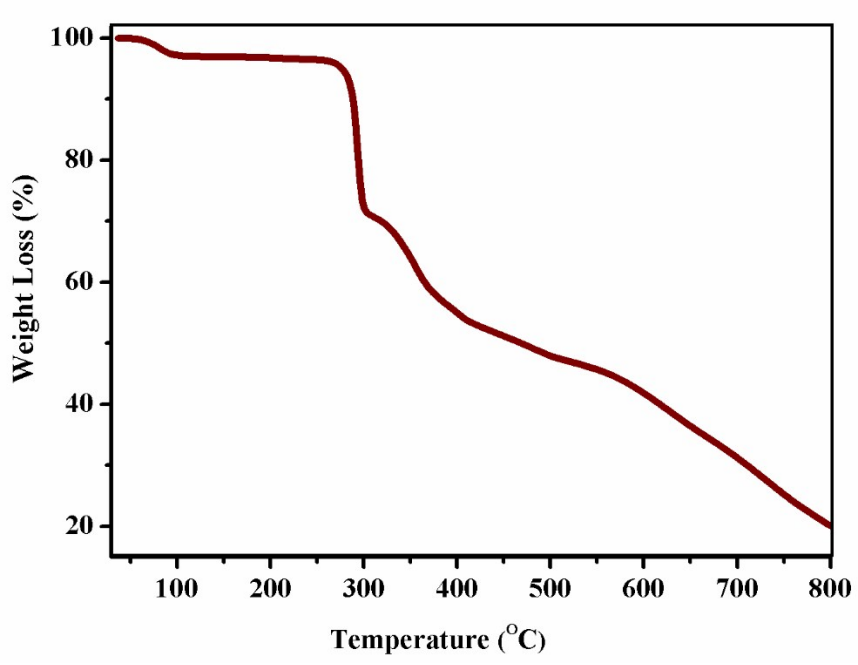

Fig. S7 Thermo gravimetric analysis profile of **Cd-MOF-1**

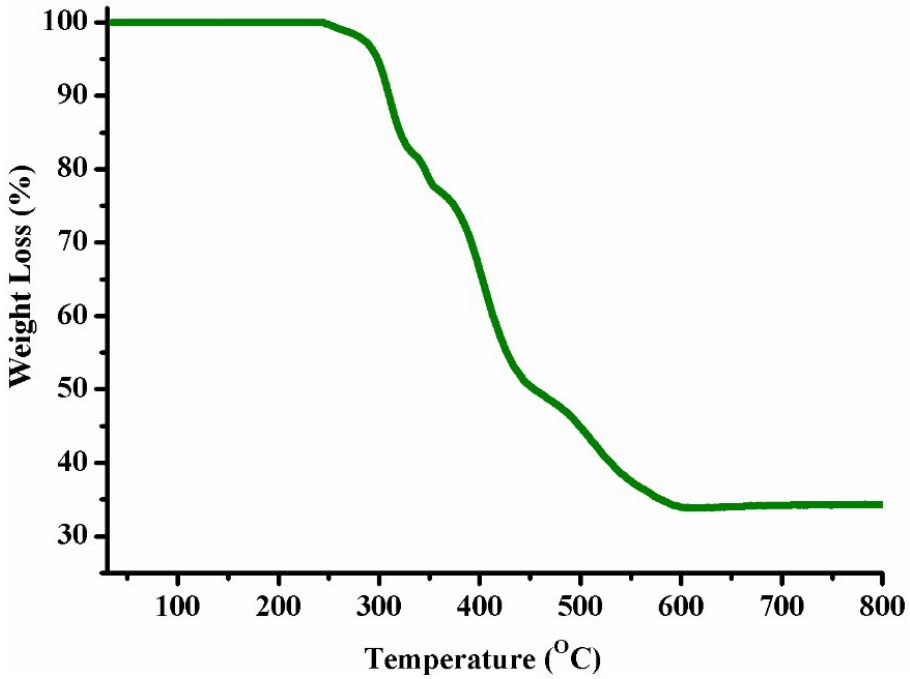

Fig. S8 Thermo gravimetric analysis profile of **Cd-MOF-2**

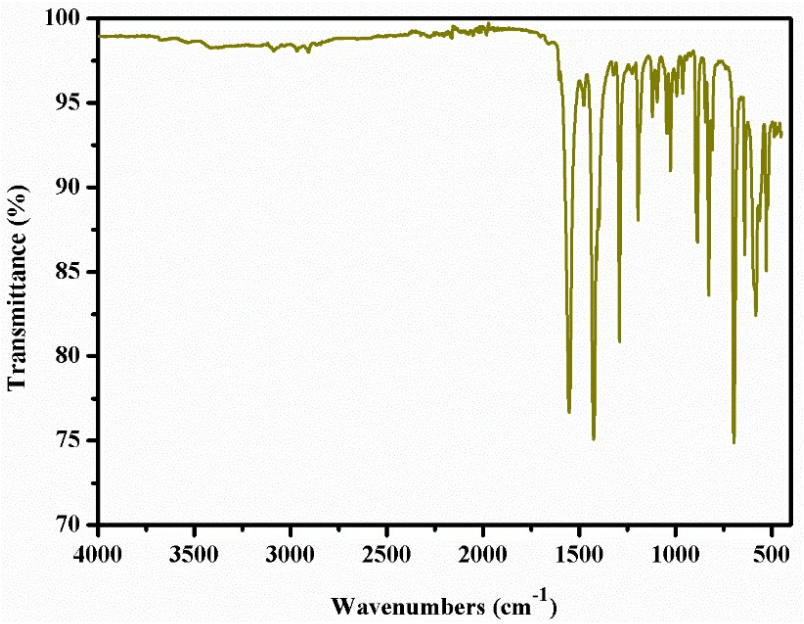

Fig. S9 FT-IR spectra of **Cd-MOF-1**.

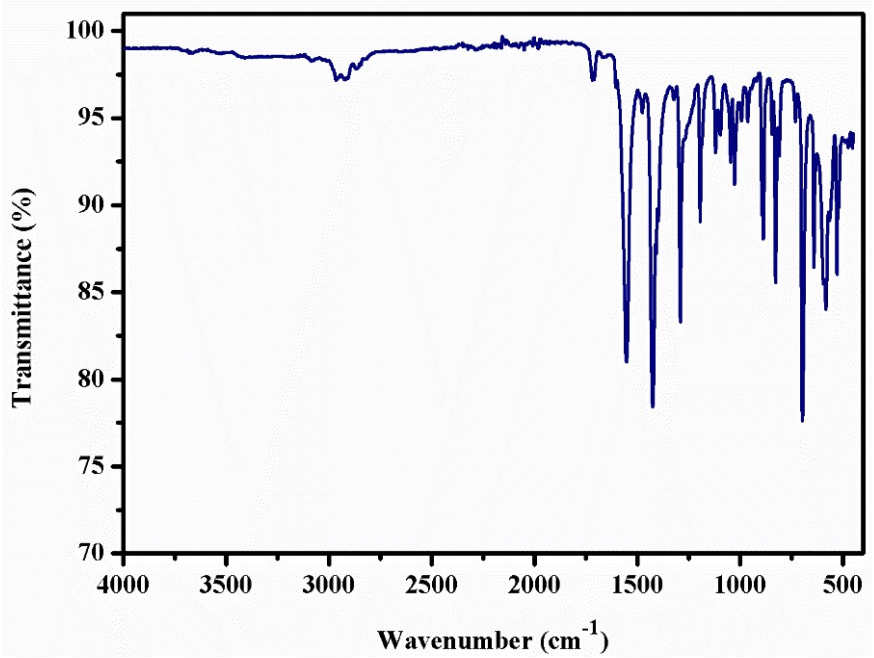

Fig. S10 FT-IR spectra of **Cd-MOF-2**

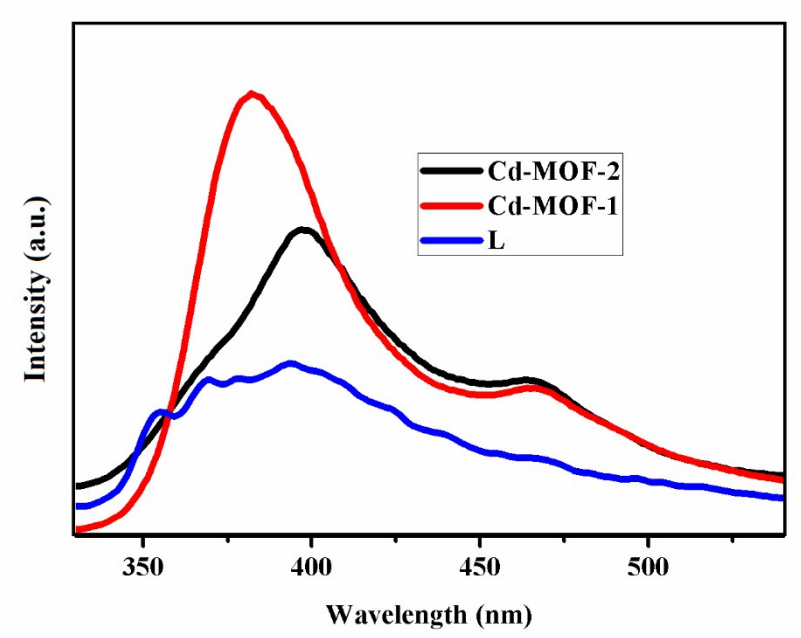

Fig. S11 The solid state emission spectra of **Cd-MOF-1** (red, λ_{ex} = 305 nm), **Cd-MOF-2** (black, λ_{ex} = 312 nm) and the spacer L (blue, λ_{ex} = 300 nm) at room temperature.

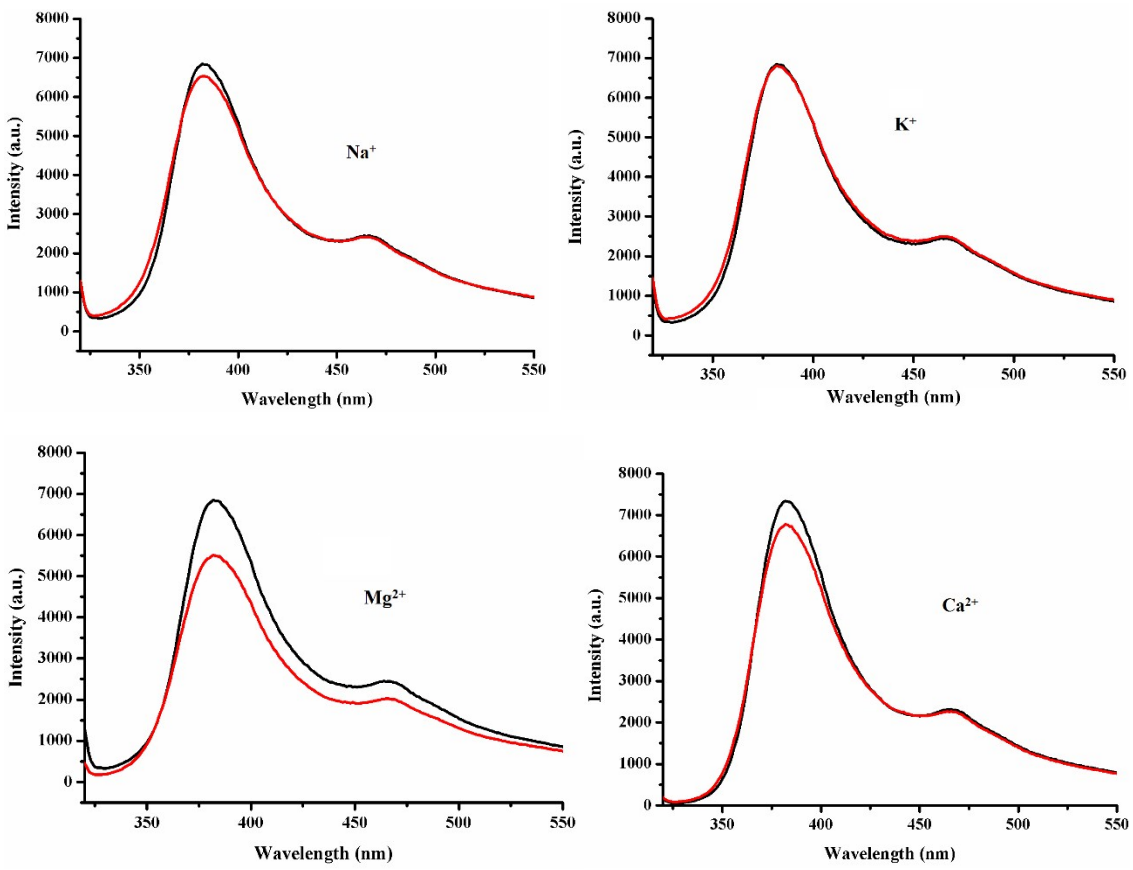

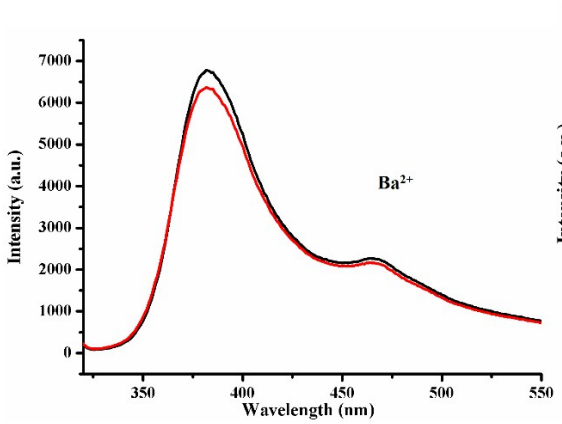
Ba2+
Intensity (a.u.)
Wavelength (nm)

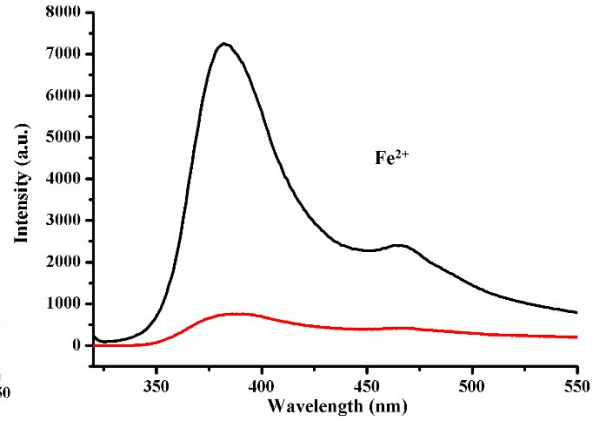
Fe2+
Intensity (a.u.)
Wavelength (nm)

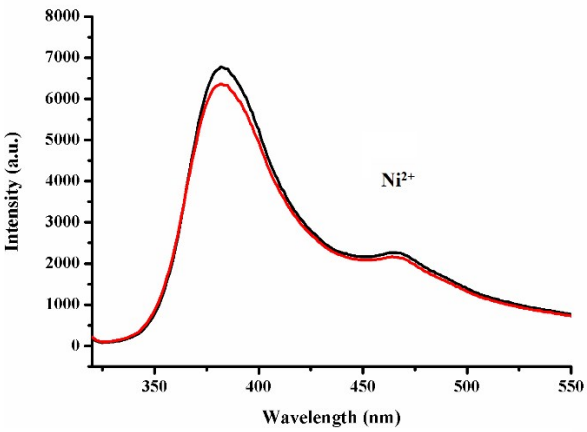
Ni2+
Intensity (a.u.)
Wavelength (nm)

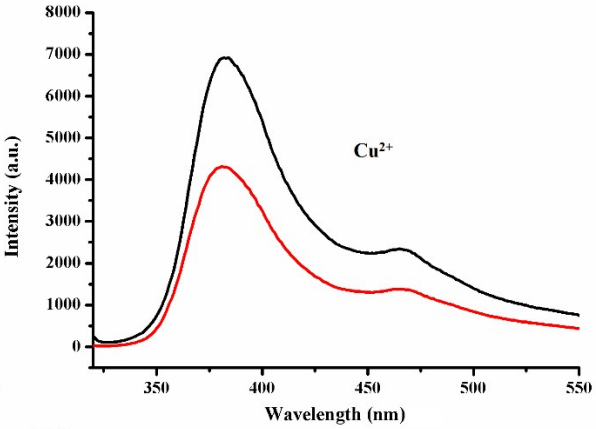
Cu2+
Intensity (a.u.)
Wavelength (nm)

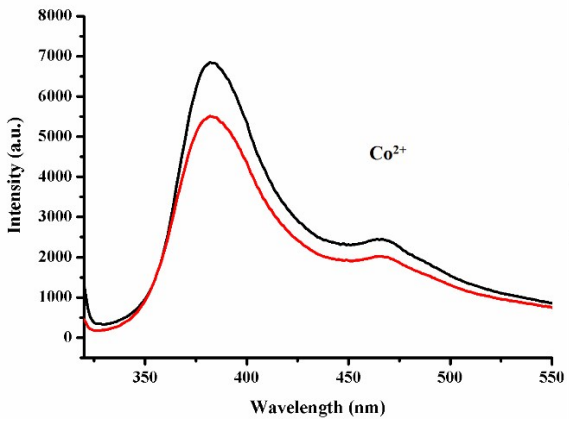
Co2+
Intensity (a.u.)
Wavelength (nm)

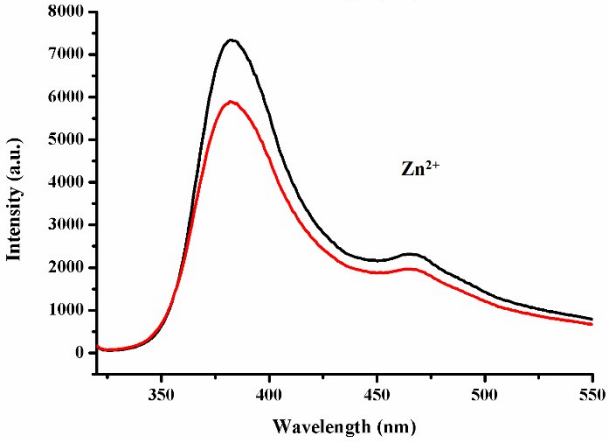
Zn2+
Intensity (a.u.)
Wavelength (nm)

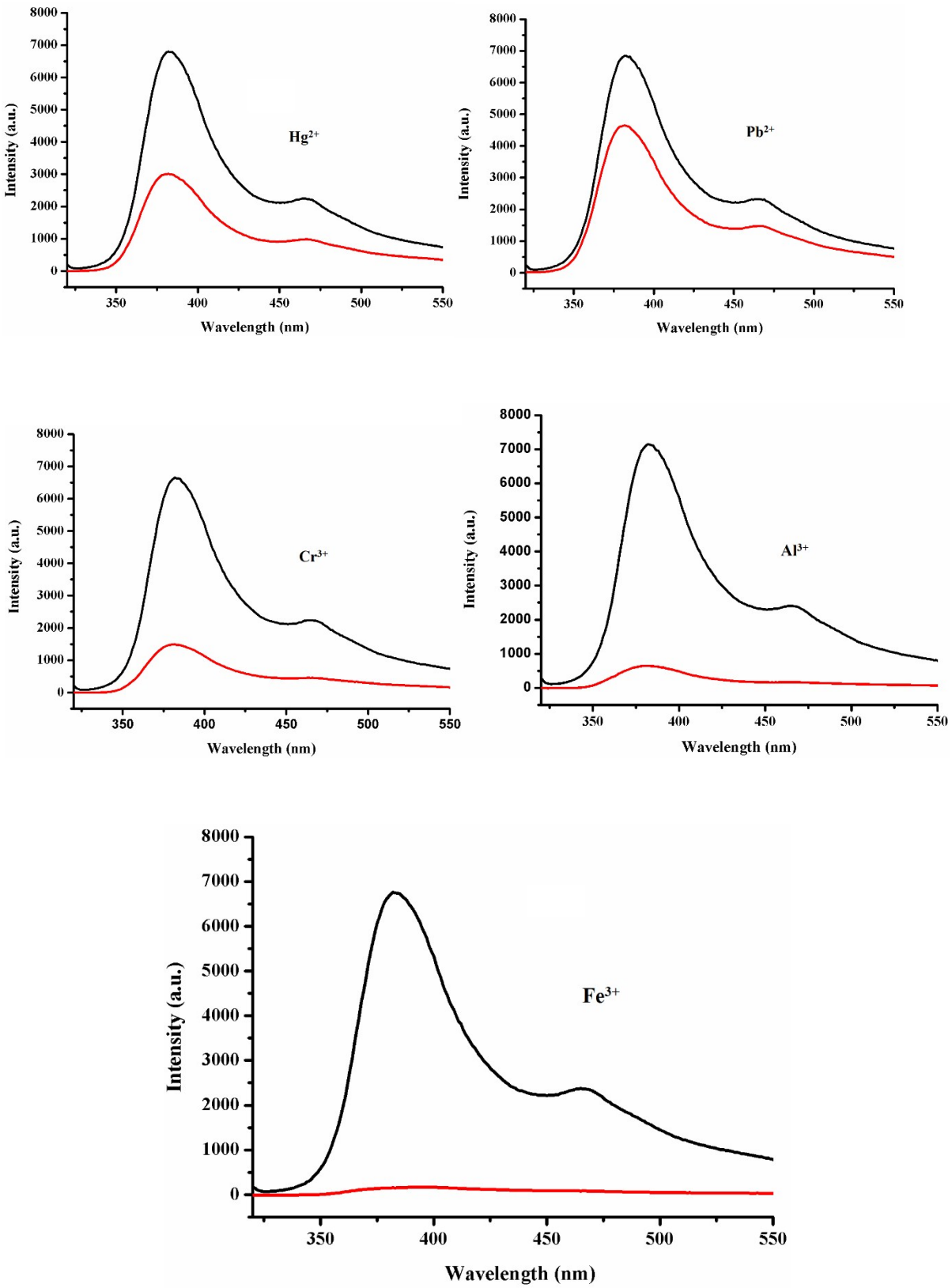

Fig. S12 The fluorescence spectra of **Cd-MOF-1** in DMF solution upon the addition of 100 μL of 10^{-2} mol/L of various metal ions.

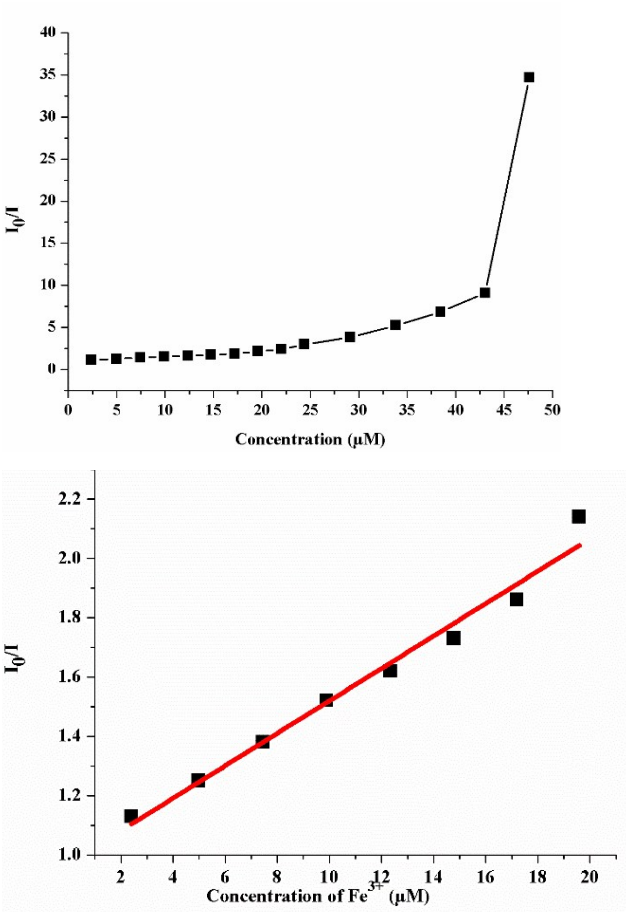

Fig. S13 Stern-Volmer plot of **Cd-MOF-1** by gradual addition of Fe^{3+} ions (left). The plot (right) demonstrate the quenching linearity relationship at low concentrations of Fe^{3+} ion.

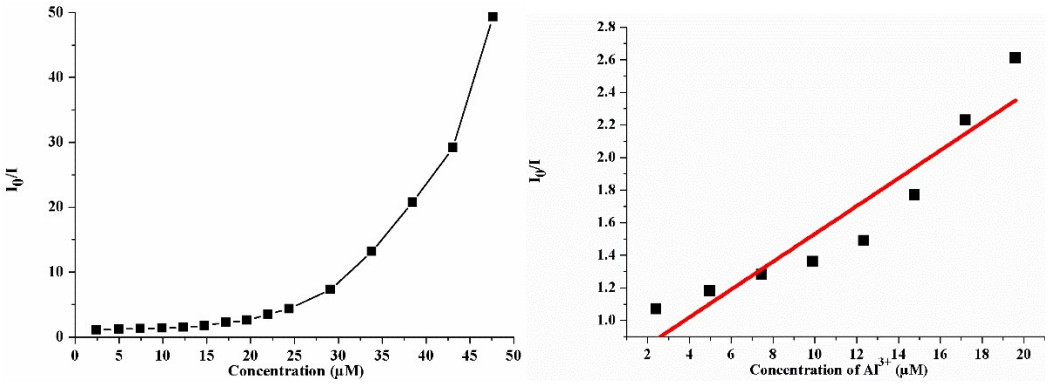

Fig. S14 Stern-Volmer plot of **Cd-MOF-1** by gradual addition of Al^{3+} ions (left). The plot (right) demonstrate the quenching linearity relationship at low concentrations of Al^{3+} ion.

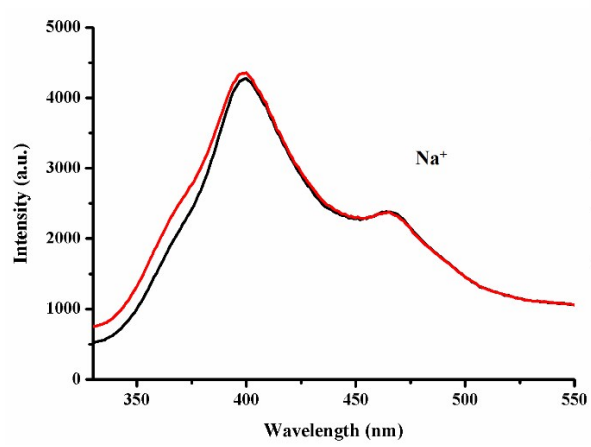
Intensity (a.u.)
Wavelength (nm)
Na+

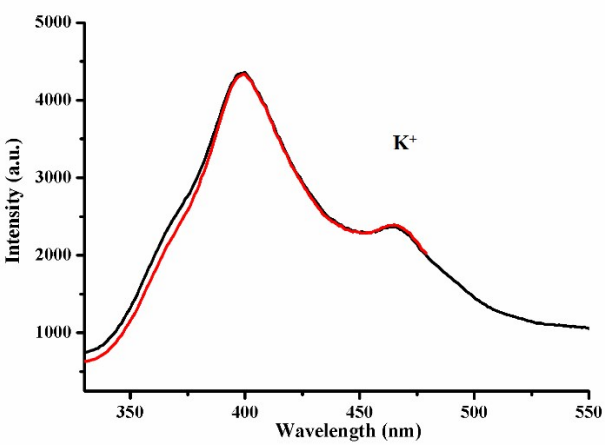
Intensity (a.u.)
Wavelength (nm)
K+

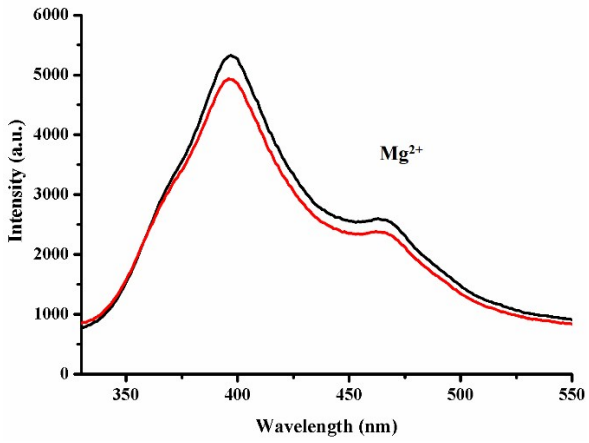
Intensity (a.u.)
Wavelength (nm)
Mg2+

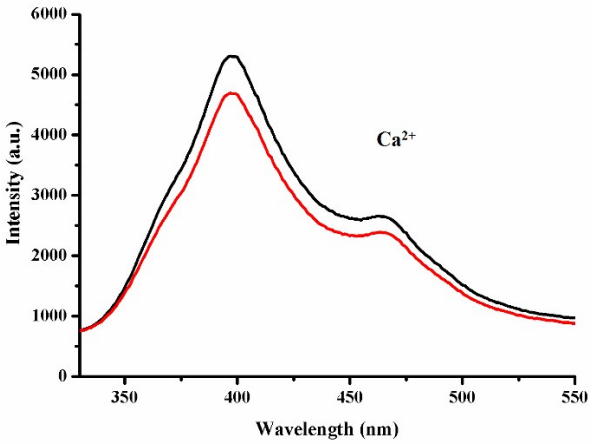
Intensity (a.u.)
Wavelength (nm)
Ca2+

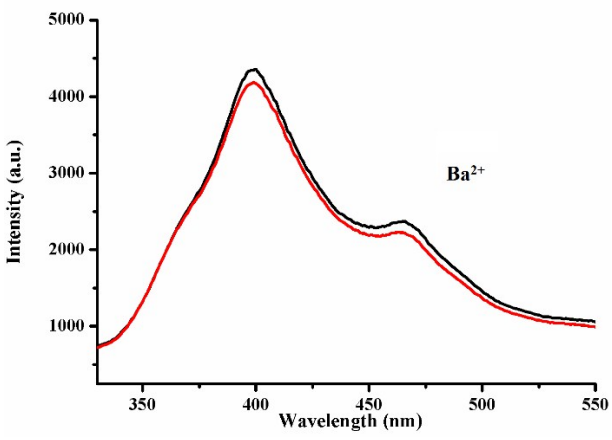
Intensity (a.u.)
Wavelength (nm)
Ba2+

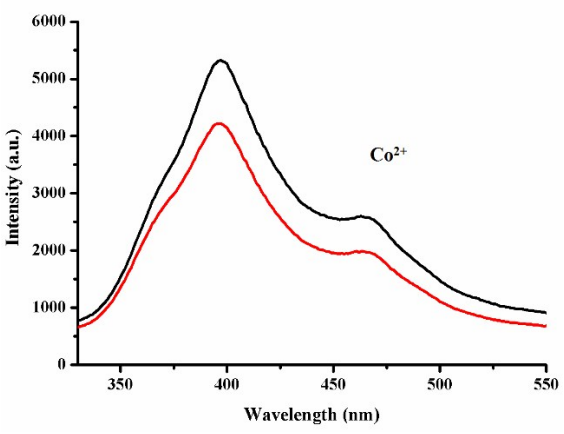
Intensity (a.u.)
Wavelength (nm)
Co2+

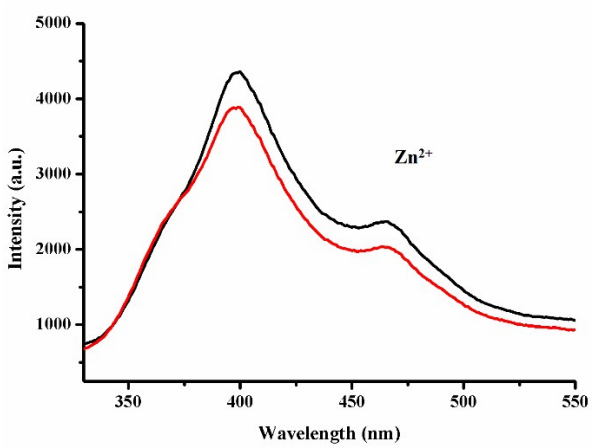
Zn2+
Intensity (a.u.)
Wavelength (nm)

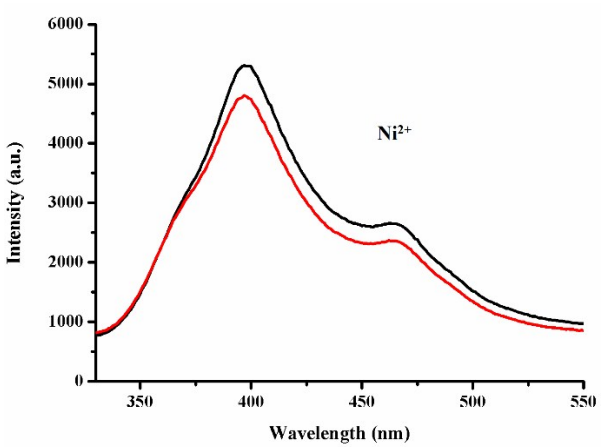
Ni2+
Intensity (a.u.)
Wavelength (nm)

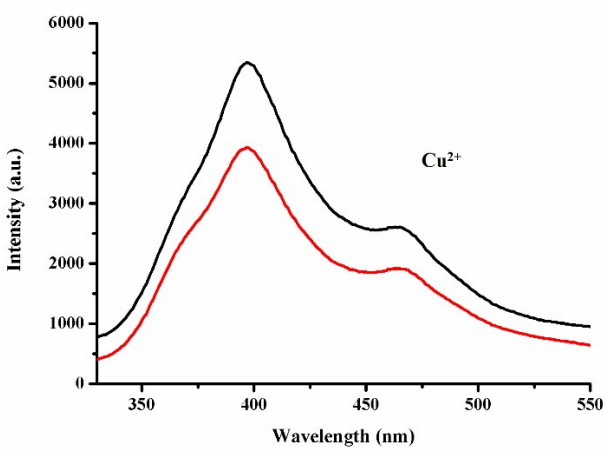
Cu2+
Intensity (a.u.)
Wavelength (nm)

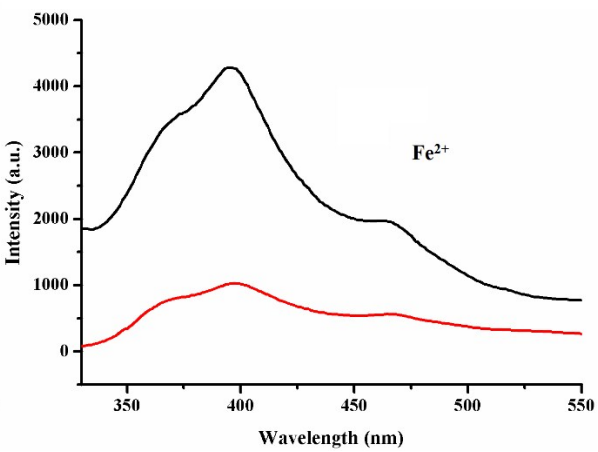
Fe2+
Intensity (a.u.)
Wavelength (nm)

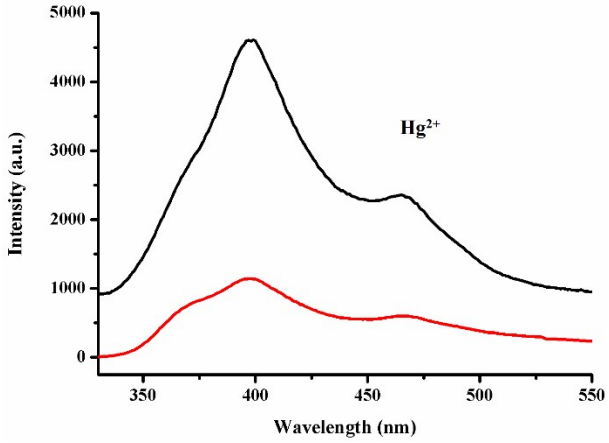
Hg2+
Intensity (a.u.)
Wavelength (nm)

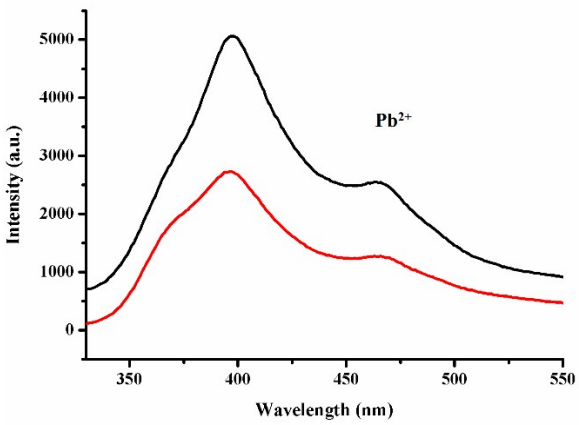
Pb2+
Intensity (a.u.)
Wavelength (nm)

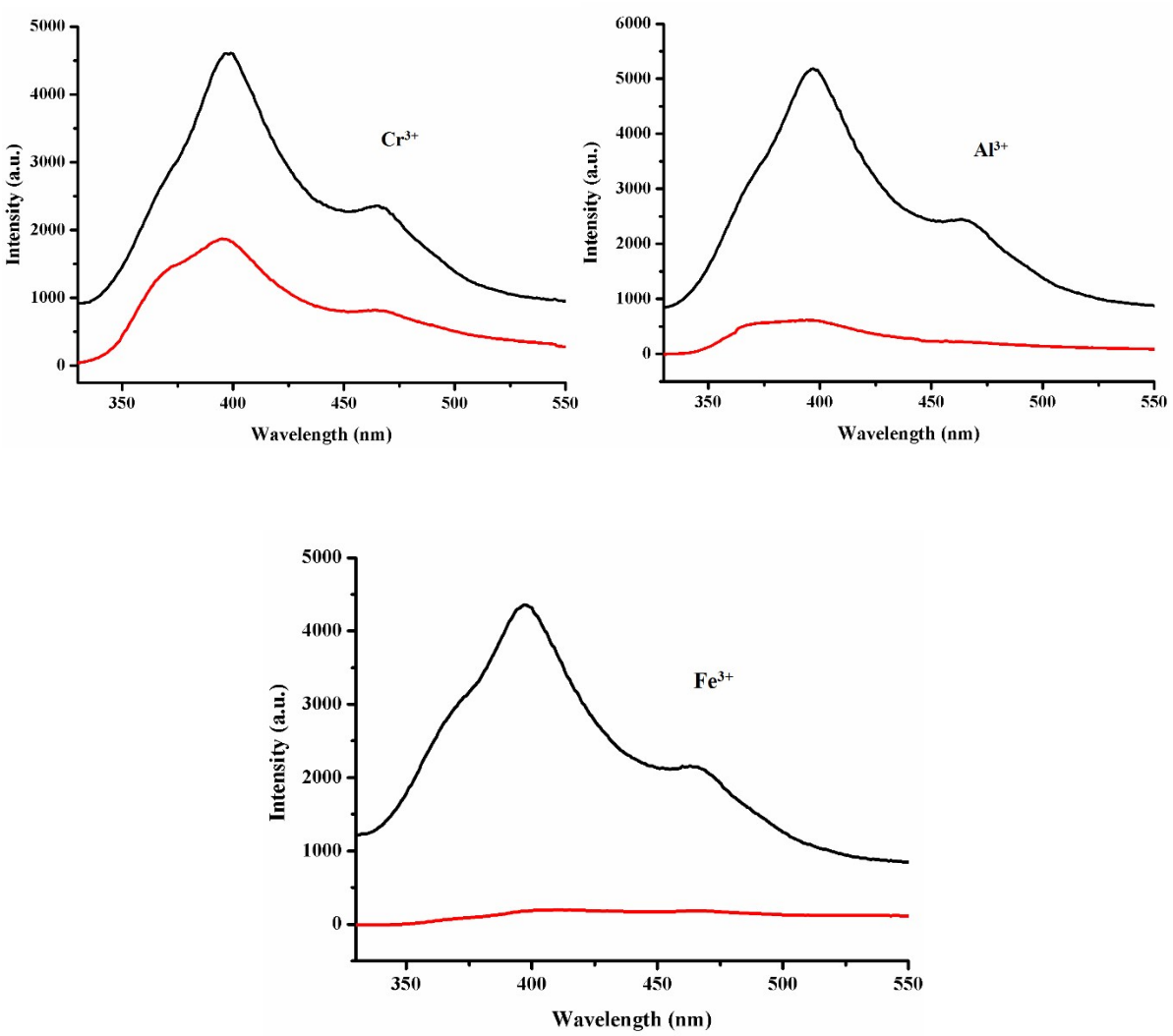

Fig. S15 The fluorescence spectra of **Cd-MOF-2** in DMF solution upon the addition of 100 μL of 10^{-2} mol/L of various metal ions.

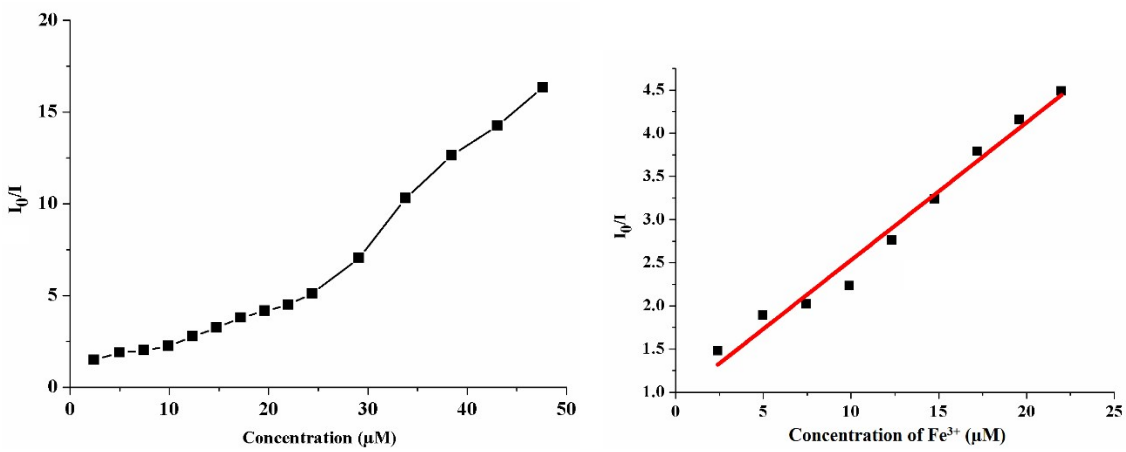

Fig. S16 Stern-Volmer plot of **Cd-MOF-2** by gradual addition of Fe^{3+} ions (left). The plot (right) demonstrate the quenching linearity relationship at low concentrations of Fe^{3+} ion.

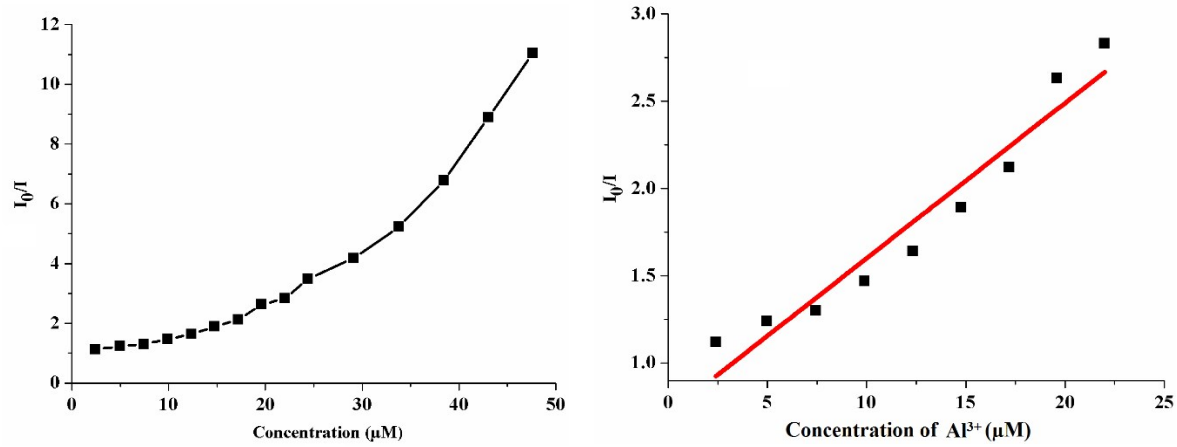

Fig. S17 Stern-Volmer plot of **Cd-MOF-2** by gradual addition of Al^{3+} ions (left). The plot (right) demonstrate the quenching linearity relationship at low concentrations of Al^{3+} ion.

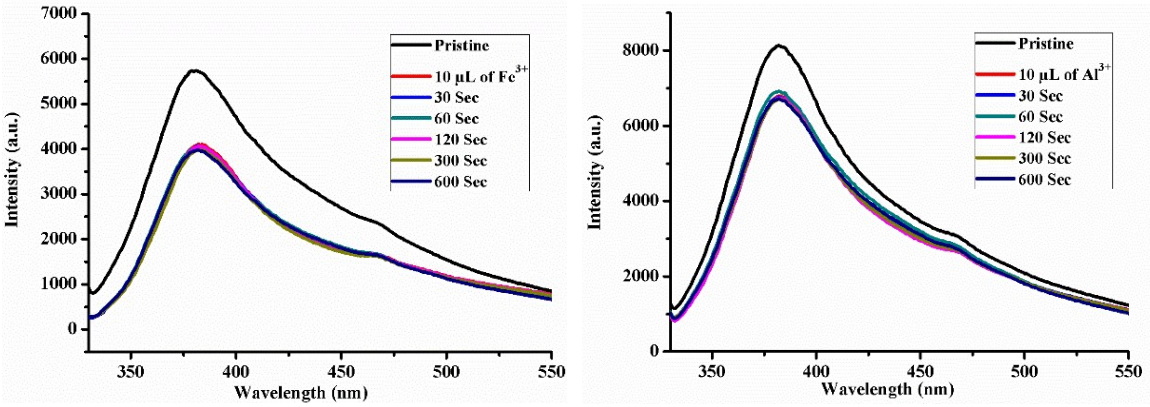

Fig. S18 Fluorescent spectra of time-dependent **Cd-MOF-1** after addition of 10 µL Fe^{3+}/Al^{3+} aqueous.

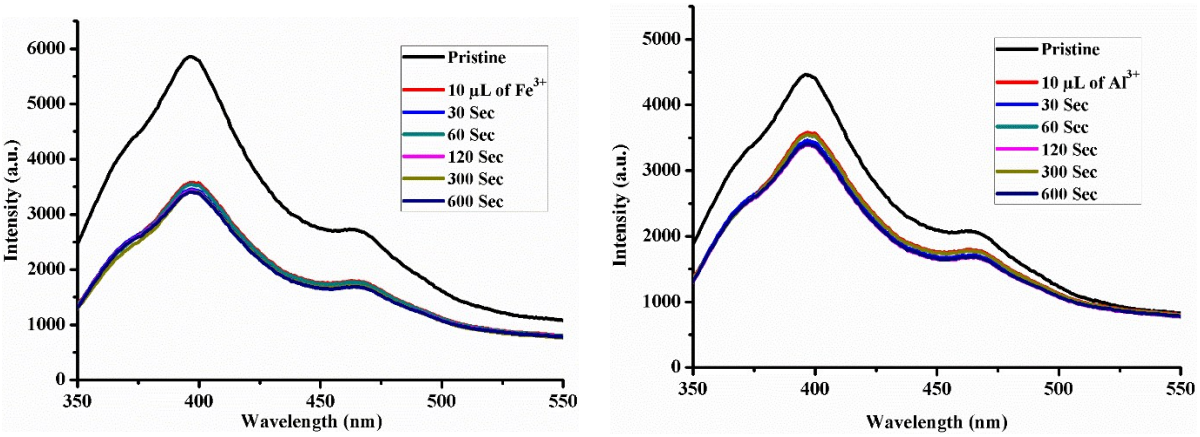

Fig. S19 Fluorescent spectra of time-dependent **Cd-MOF-2** after addition of 10 µL Fe^{3+}/Al^{3+} aqueous solutions.

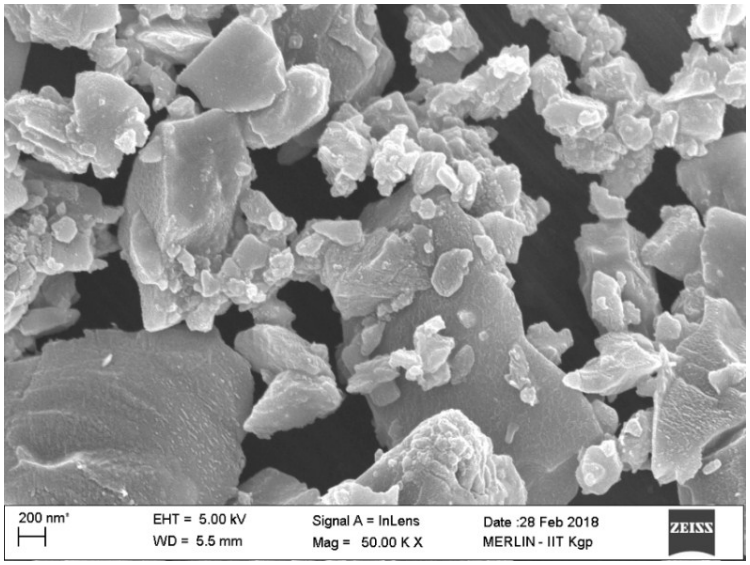

Fig. S20 (a) SEM image of the morphology of **Cd-MOF-1** after loading Fe^{3+}.

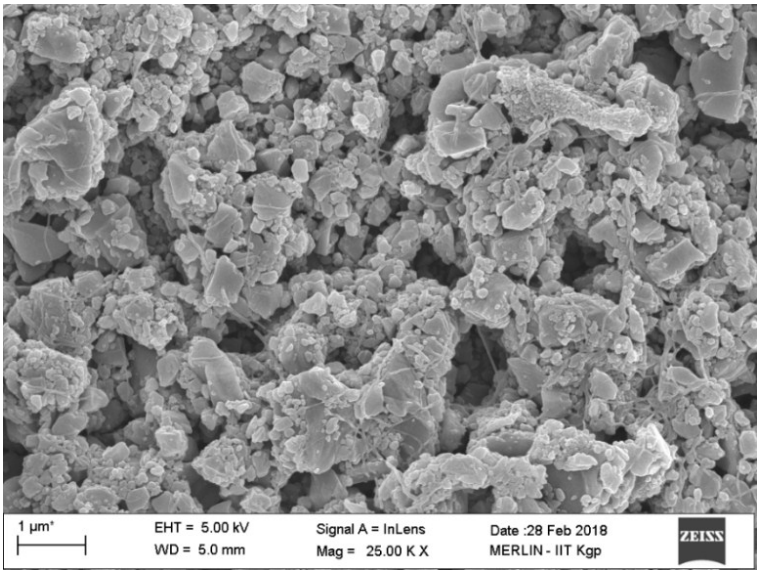

Fig. S21 (a) SEM image of the morphology of **Cd-MOF-2** after loading Fe^{3+}.

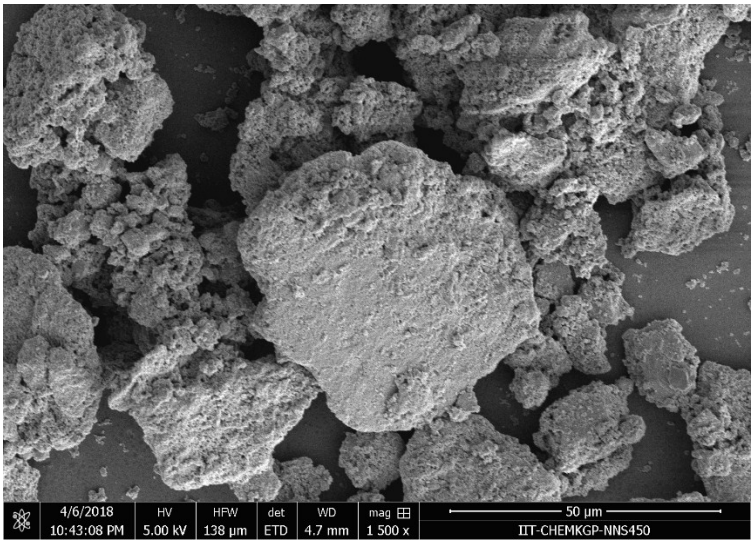

Fig. S22 (a) SEM image of the morphology of **Cd-MOF-1** after loading Al^{3+}.

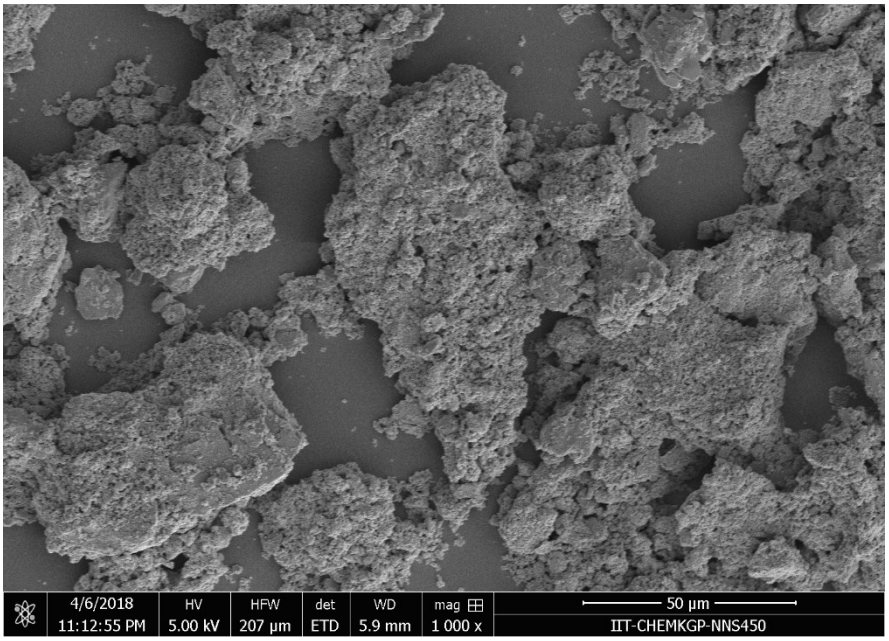

Fig. S23 (a) SEM image of the morphology of **Cd-MOF-2** after loading Al^{3+}.

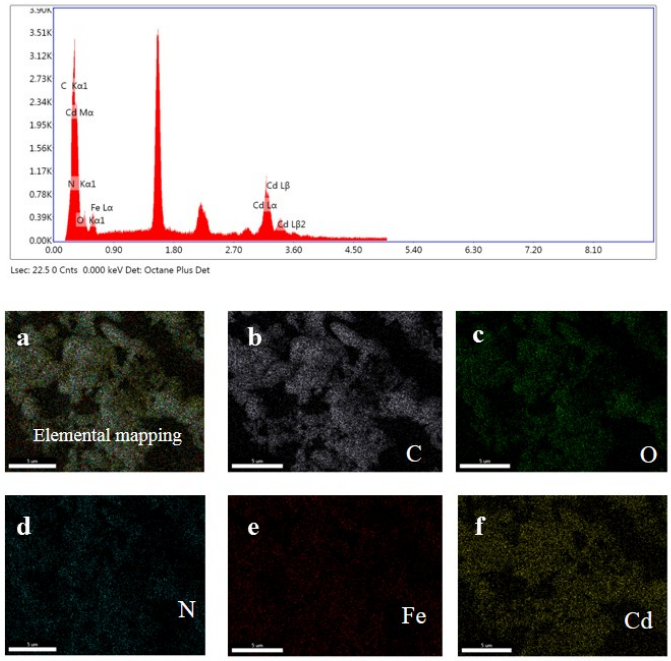

Fig. S24 EDX mapping of **Cd-MOF-1** after loading Fe^{3+}. (a) Overlapped element mapping; (b) C element mapping; (c) N element mapping; (d) O element mapping; (e) Cd element mapping; (f) Fe element mapping.

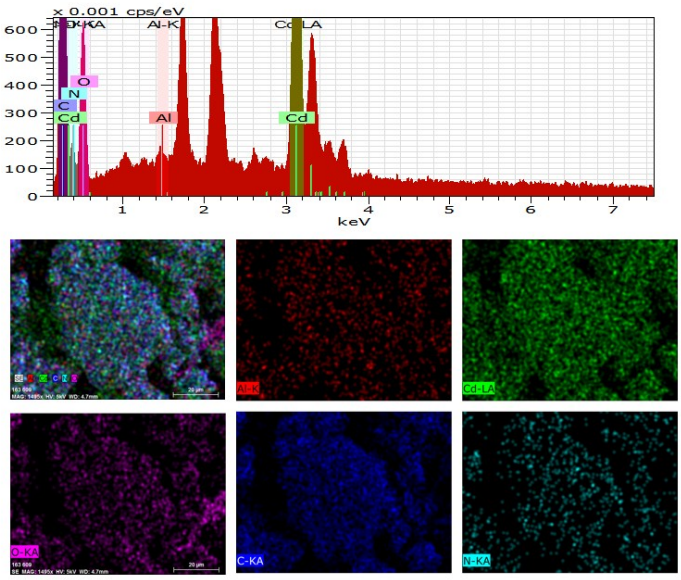

Fig. S25 EDX mapping of **Cd-MOF-1** after loading Al^{3+} (above); Overlapped and individual element mapping (bellow).

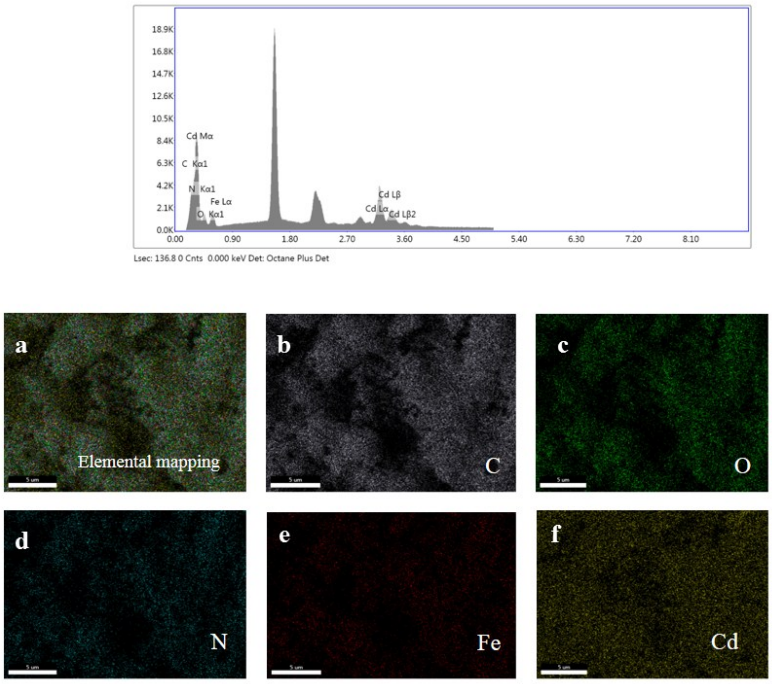

Fig. S26 EDX mapping of **Cd-MOF-2** after loading Fe^{3+}. (a) Overlapped element mapping; (b) C element mapping; (c) N element mapping; (d) O element mapping; (e) Cd element mapping; (f) Fe element mapping.

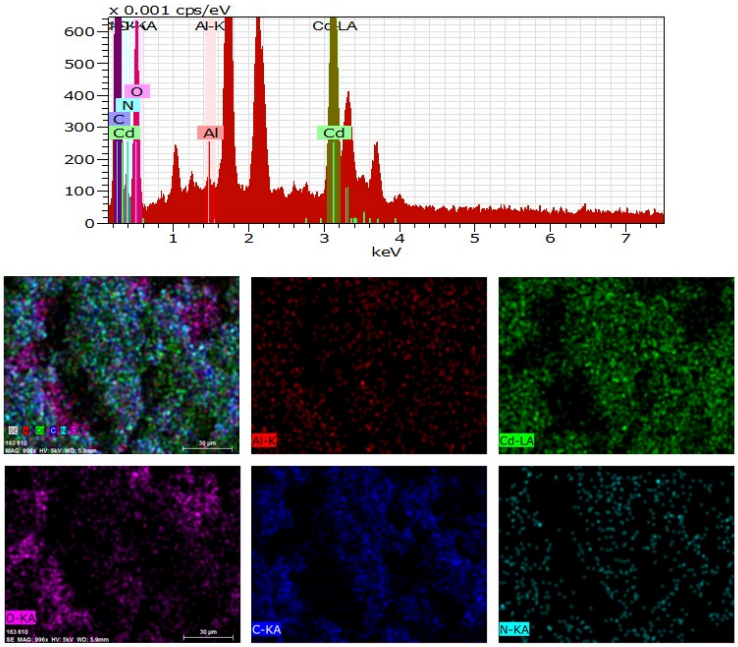

Fig. S27 EDX mapping of **Cd-MOF-2** after loading Al^{3+} (above); Overlapped and individual element mapping (bellow).

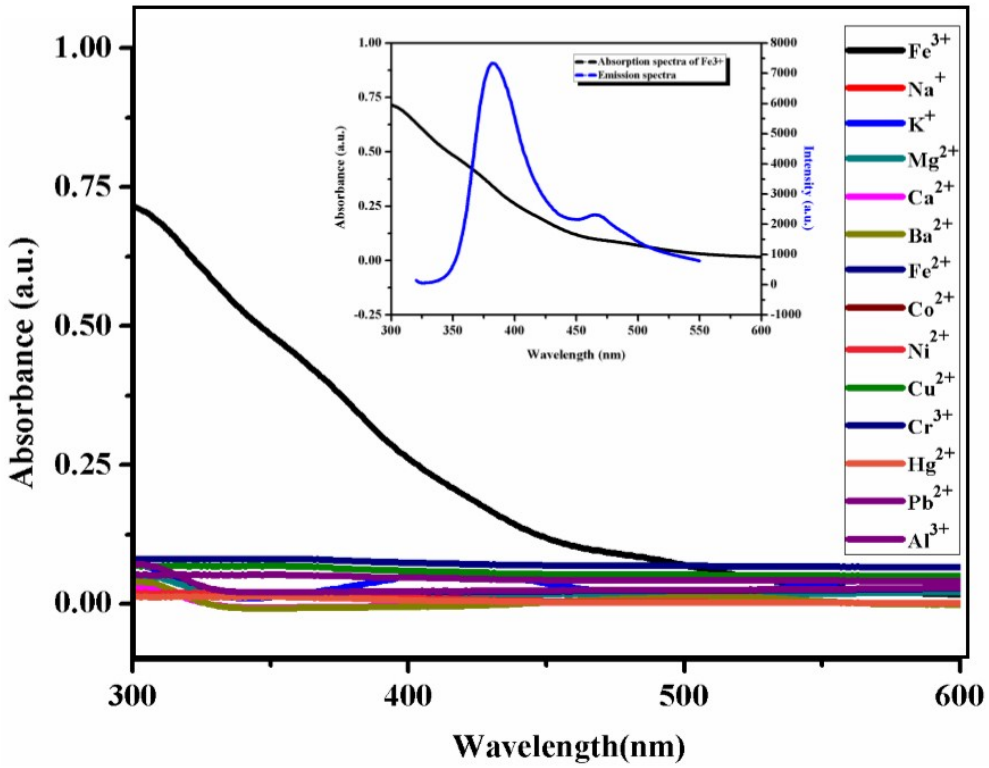

Fig. S28 UV-Vis absorption spectra of different metal ions. In the inset, the emission spectrum of **Cd-MOF-1** and the absorption spectra of Fe^{3+} ion.

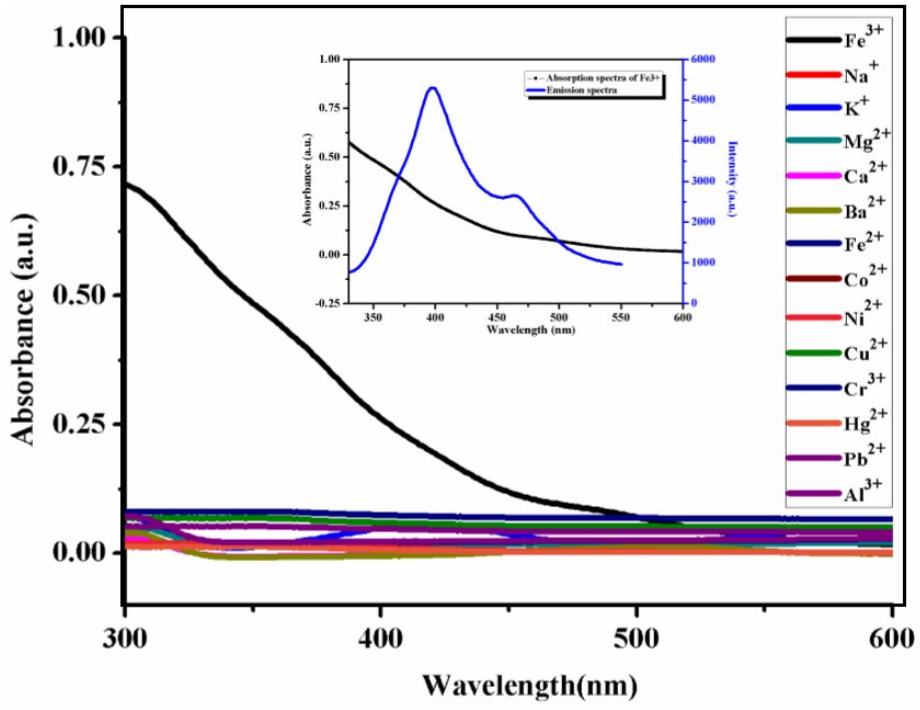

Fig. S29 UV-Vis absorption spectra of different metal ions. In the inset, the emission spectrum of **Cd-MOF-2** and the absorption spectra of Fe^{3+} ion.

Table S2: Selected Bond Distances (Å) and Bond Angles (°) in **Cd-MOF-1**.

Cd1	O1	2.519(4)	Cd1	O2	2.330(4)	Cd1	N1	2.355(5)
Cd1	O4	2.400(4)	Cd1	O5	2.343(4)	Cd1	N8	2.350(5)
Cd1	O3	2.380(4)	Cd2	O5	2.367(4)	Cd2	N4	2.369(5)
Cd2	O2	2.330(4)	Cd2	O6	2.492(4)	Cd2	O7	2.357(4)
Cd2	O8	2.418(5)	Cd2	N5	2.353(5)			

O3	Cd1	O1	91.88(14)	O5	Cd1	O1	125.68(14)	
O5	Cd1	O3	142.26(14)	O4	Cd1	O1	146.46(14)	
O4	Cd1	O3	54.89(14)	O4	Cd1	O5	87.81(15)	
O2	Cd1	O1	53.56(14)	O2	Cd1	O3	145.07(14)	
O2	Cd1	O5	72.13(15)	O2	Cd1	O4	159.94(15)	
N8	Cd1	O1	90.46(15)	N8	Cd1	O3	84.78(16)	
N8	Cd1	O5	90.79(16)	N8	Cd1	O4	90.81(17)	
N8	Cd1	O2	90.00(17)	N1	Cd1	O1	90.70(16)	
N1	Cd1	O3	97.02(16)	N1	Cd1	O5	87.03(16)	
N1	Cd1	O4	89.24(17)	N1	Cd1	O2	89.20(17)	
N1	Cd1	N8	177.82(16)	O5	Cd2	O6	53.65(14)	
O7	Cd2	O6	92.29(14)	O7	Cd2	O5	145.50(14)	
O8	Cd2	O6	147.17(14)	O8	Cd2	O5	159.18(15)	
O8	Cd2	O7	55.08(15)	O2	Cd2	O6	125.29(14)	
O2	Cd2	O5	71.70(15)	O2	Cd2	O7	142.31(15)	
O2	Cd2	O8	87.50(15)	N4	Cd2	O6	88.61(16)	

N4	Cd2	O5	88.04(16)	N4 Cd2 O7	85.53(16)
N4	Cd2	O8	91.93(17)	N4 Cd2 O2	92.02(17)
N5	Cd2	O6	89.21(16)	N5 Cd2 O5	88.41(16)
N5	Cd2	O7	97.36(16)	N5 Cd2 O8	91.42(17)
N5	Cd2	O2	86.95(17)	N5 Cd2 N4	176.45(17)

Table S3: Non-bonding interactions in **Cd-MOF-1**.

D	H…A	d(H…A) (Å)	D(D…A) (Å)	< DHA (^{O})
C2	H2…O1	2.414(4)	3.220(5)	144.82(7)
C8	H8…O7	2.504(4)	3.011(5)	114.55(7)
C9	H9…O8	2.657(4)	3.343(5)	130.96(7)
C12	H12…O6	2.364(2)	3.189(3)	147.58(10)
C17	H17…O3	2.699(3)	3.054(4)	103.57(12)
C18	H18…O3	2.653(3)	3.040(4)	105.70(10)
C19	H19…O4	2.574(3)	3.254(3)	130.34(8)

Table S4: Selected Bond Distances (Å) and Bond Angles (^{o}) in **Cd-MOF-2**.

Cd1	O1	2.2664(15)	Cd1 O2	2.2685(14)	Cd1	N1	2.3143(16)
Cd1	O4	2.3060(15)	Cd1 N4	2.3193(15)	Cd1	O3	2.4560(14)

O1	Cd1	O2	126.56(5)	O1 Cd1 O4	140.89(5)
O2	Cd1	O4	92.52(6)	O1 Cd1 N1	91.24(6)

O2	Cd1	N1	92.63(5)	O4	Cd1	N1	84.79(6)
O1	Cd1	N4	85.83(5)	O2	Cd1	N4	84.66(5)
O4	Cd1	N4	101.01(6)	N1	Cd1	N4	173.68(5)
O1	Cd1	O3	86.46(5)	O2	Cd1	O3	146.94(5)
O4	Cd1	O3	54.57(5)	N1	Cd1	O3	87.83(5)
N4	Cd1	O3	97.56(5)				

Table S5: Non-bonding interactions in **Cd-MOF-2**.

D	H…A	d(H…A) (Å)	D(D…A) (Å)	< DHA (^{O})
C15	H15…O1	2.672(4)	3.206(5)	117.16(7)
C16	H16…O2	2.457(2)	3.073(3)	123.85(10)
C18	H18…O3	2.301(3)	3.147(4)	150.99(12)
C10	H10…O4	2.128(3)	2.996(4)	154.91(10)

Table S6. A comparison of MOF-based luminescent probes for the detection of Fe^{3+} ions.

Fluorescent Material	K_{sv} value (L/M^{-1})	Reference
$\{[Tb_4(OH)_4(DSOA)_2(H2O)_8].(H_2O)_8\}_n$	3.543×10^4	*J. Mater. Chem. A*, **2015**, *3*, 641–647
$\{(Me_2NH_2)[Tb(OBA)_2]\cdot(Hatz)\cdot(H_2O)1.5\}_n$	3.4×10^4	*J. Mater. Chem. C,* 2017, 5, 2311-2317
(MOF-LIC-1)._Eu	2.8×10^4	*J. Mater. Chem.* C, 2014, 2, 6758–6764
Cd-MOF-1	2.1×10^4	**This Work**
Eu−HODA	2.09×10^4	*Inorg. Chem.* **2016**, *55*, 12660−12668
$[Zn_2(TPOM)(NDC)_2]\cdot3.5H_2O$	1.9×10^4	*Inorg. Chem.* **2017**, *56*, 12348−12356
$[Cd_3\{Ir(ppy-$	1.165×10^4	*Inorg. Chem.* **2018**, 57,

$COO)_3\}_2(DMF)_2(H_2O)_4]\cdot 6H_2O\cdot 2DMF$		1079−1089
$[Tb(TBOT)(H_2O)](H_2O)_4(DMF)(NMP)_{0.5}$	5.51×10^3	*J. Mater. Chem. C*, **2017**, *5*, 2015–2021.
Cd-MOF-2	5.4×10^3	**This Work**
$[Zr_6O_4(OH)_4(C_8H_2O_4S_2)_6]\cdot DMF\cdot 18H_2O$	4.41×10^3	*Dalton Trans*., **2018**, *47*, 1159–1170.
$\{[Tb(TATAB)(H2O)_2]\cdot NMP\cdot H_2O\}_n$	3.6×10^3	*Dalton Trans*., **2016**, *45*, 15492–15499.
$[Zn_2(L_1)_2(bpe)_2(H_2O)_2]$	2395	*Dalton Trans*, **2015**, *44*, 18795–18803.
$Ln_3L_2(OH)(DMF)_{0.22}(H_2O)_{5.78}]\cdot$guest	393	*ChemPlusChem* **2016**, *81*, 1299−1304.

Table S7. A comparison of MOF-based luminescent probes for the detection of Al^{3+} ions.

Fluorescent Material	K_{SV} (L/mole)	Reference
$\{[Eu(BTB)(phen)]\cdot 4.5DMF\cdot 2H_2O\}_n$	1.59×10^4	*Inorg. Chem*., **2016**, *55*, 9671–9676
$\{Zn(DMA)(TBA)\}_n$	1.33×10^4	*Inorg. Chem. Front*., **2017**, *4*, 1888–1894
Cd-MOF-1	4.9×10^3	**This Work**
(TMU-34) F	4170	*Ultrasonics - Sonochemistry* **2018**, *41*, 17–26.
Cd-MOF-2	2.6×10^3	**This Work**

References:

(1) SAINT+, 6.02ed, Bruker AXS, Madison, WI, 1999.

(2) XPREP, 5.1 ed. Siemens Industrial Automation Inc., Madison, WI, 1995.

(3) G. M. Sheldrick, *SHELXTL ™Reference Manual*: version 5.1, Bruker AXS, Madison, WI, 1997.

(4) G. M. Sheldrick, Crystal Structure Refinement with SHELXL. *Acta Cryst C*, 2015, **71**, 3–8.

(5) A. L. Spek, Single-crystal Structure Validation with the Program PLATON. *J. Appl. Crystallogr*. 2003, **36**, 7−13.